1985ApJ...298..114M

THE ASTROPHYSICAL JOURNAL, 298:114–127, 1985 November 1
© 1985. The American Astronomical Society. All rights reserved. Printed in U.S.A.

MODELS FOR HIGH-FREQUENCY RADIO OUTBURSTS IN EXTRAGALACTIC SOURCES, WITH APPLICATION TO THE EARLY 1983 MILLIMETER-TO-INFRARED FLARE OF 3C 273

ALAN P. MARSCHER
Department of Astronomy, Boston University

AND

WALTER K. GEAR
School of Physics and Astronomy, Lancashire Polytechnic
Received 1984 December 3; accepted 1985 April 26

ABSTRACT

We present models for the variability of compact radio sources with specific application to the early 1983 millimeter-to-infrared flare of the quasar 3C 273. We show that the early evolution of the outburst spectrum is most readily explained if the flaring component is expanding. In our models the effects of individual events are first detected in the millimeter-to-infrared region of the spectrum, as observed in 3C 273. The models include the effects of synchrotron, Compton, and expansion losses as well as variable injection of relativistic electrons and magnetic field. We find that a model based on a uniform expanding source requires rather artificial variations of particle injection with source radius if it is to explain the 3C 273 flare data presented by Robson *et al.* The observed behavior is obtained in a more natural way by a second model in which the outburst is due to a shock wave passing through an adiabatic, conical, relativistic jet. We extend the application of this model by showing that it can reproduce many of the characteristics of general radio source variability. The model can also naturally explain the production and evolution of superluminal knots on VLBI maps and their tendency to collectively form relatively flat radio spectra, as well as the variable X-ray emission observed from 3C 273 and other similar sources. The minimum time scale of variability can be as short as ~ 1 day, despite the rather large distance ($\gtrsim 1$ pc) of the shock from the central energy source of the quasar.

Subject headings: quasars — radiation mechanisms — radio sources: variable

I. INTRODUCTION

It has long been known that compact radio sources tend to be variable at all wavelengths (see, e.g., Kellermann and Pauliny-Toth 1981), although the relation or correlation of variations at different wavelengths is often far from clear (see, e.g., Epstein *et al.* 1982). In general, however, the radio variations begin at high frequencies and propagate to low frequencies (e.g., O'Dea, Dent, and Balonek 1984), with amplitudes of variation which are inconsistent with the simple expanding cloud model of van der Laan (1966) and Pauliny-Toth and Kellermann (1966).

A major problem of radio variability studies is that the mean time beteeen events is often less than the decay time of each event. This makes it very difficult to separate the bursting component from any more slowly varying ("quiescent") emission that may be present.

Milliarcsecond-scale VLBI maps of 3C 273 reveal the presence of a compact "core" from which emerges a succession of knots which separate from the core at superluminal speeds while diminishing in brightness (Unwin *et al.* 1985). The data are consistent with the core having roughly constant flux density, only appearing to brighten when blended (within the resolution of the VLBI map) with a new knot. (It has recently been demonstrated that the core of a similar object, 3C 345, is stationary to within the experimental errors [Bartel *et al.* 1984]). However, the VLBI maps may not always reveal the "naked" core: a blended, newly born knot often contaminates the core emission by the time the previous knot has separated sufficiently from the core to be identified. Because of these complications, the *possibly* constant core flux density cannot be reliably determined at centimetric wavelengths. Furthermore, the knots are typically decaying in flux density by the time they are separated from the core on VLBI maps; by this time we have missed the most interesting period of their evolution.

In order to resolve these problems, it is necessary to make observations at wavelengths shorter than the radio range, namely, millimeter, submillimeter, and infrared wavelengths. For most compact, variable sources, the transition from the flat, partially opaque radio spectrum to the steep, optically thin IR/optical continuum occurs in the millimeter-to-submillimeter region of the spectrum (see, e.g., Gear *et al.* 1985*a*). Emission at these frequencies therefore arises in *the most compact* region of the radio source.

The submillimeter and far-IR properties of compact radio sources were entirely unknown until very recently. Clegg *et al.* (1983) measured the flux density of 3C 273 for the first time at 100, 240, 380, and 770 μm, as well as at 1.1, 2.0, 3.3, and 8.9 mm. They showed that the flat radio spectrum breaks at ~ 60 GHz to a log-log slope of -0.7 which extends through the millimeter, submillimeter, and far-IR regions of the spectrum. The fact that this spectrum can be extrapolated smoothly to the IR measurements of Neugebauer *et al.* (1978) suggests that it represents the "quiescent" emission of 3C 273. Gear *et al.* (1984) also show that the 1.1 mm flux density from 3C 273 did not vary significantly over the period 1980–1982, while Backer (1984) finds that the 90 GHz flux density measured by Clegg *et al.* represents a minimum in the light curve. Neugebauer *et al.* also show that the 2.2 μm flux

© American Astronomical Society • Provided by the NASA Astrophysics Data System

1985ApJ...298..114M

density did not vary significantly over the period 1967–1977. These observations suggest that the time scale of variability of the quiescent emission is of the order of at least several years.

In 1983, however, there was a dramatic outburst in the millimeter-to-IR emission from 3C 273 (reported in Robson *et al.* 1983). The properties of this outburst are discussed in § II. In our interpretation of this flare, given in § III, we substract the quiescent spectrum given in Clegg *et al.* (1983) from the flux densities reported in Robson *et al.* to obtain the spectrum of the time-varying component. Here we present a theoretical analysis of this component. We find that, while a contrived uniform, expanding source model can reproduce the primary properties of the flare, a new model involving a shock in a relativistic jet can do so in a more natural way. We suggest that such a model can be applied in general to high-frequency radio outbursts in extragalactic radio sources (Gear *et al.* 1985*b*).

II. PROPERTIES OF THE EARLY 1983 MILLIMETER-TO-INFRARED FLARE OF 3C 273

We adopt the working hypothesis that the spectrum presented by Clegg *et al.* (1983) represents emission whose time scale of variability is considerably greater than that of the flaring component(s). The steeper spectral slope recorded for the early 1983 spectra, along with the disappearance of the break at 3 μm, lends support to this hypothesis. As final evidence, we also note that the IR emission returned almost exactly to the level of the "quiescent" emission after a period of a few months.

The spectral properties of this quiescent emission from 3C 273 have been established by Clegg *et al.* (1983). The spectral slope α ($S \propto \nu^{\alpha}$) is -0.7 from about 10^{11} to 10^{14} Hz. Below 10^{11} Hz, the spectrum flattens into the radio. As is indicated by the centimeter-wavelength VLBI maps (Unwin *et al.* 1985), this results from the superposition of the self-absorbed spectra of the core and several superluminal knots (model A of Clegg *et al.*). The spectrum steepens above 10^{14} Hz, then becomes dominated at optical frequencies by another component with a flatter spectrum (e.g., Neugebauer *et al.* 1979; Shields 1978), which Malkan and Sargent (1982) attribute to thermal emission from an accretion disk.

The spectrum of the early 1983 flaring component, obtained by a subtraction of the early 1982 quiescent spectrum of Clegg *et al.* (1983) from the outburst data measured by Robson *et al.* (1983), is given in Figure 1 for epochs 1983 February 2–6 and March 4–7. The excellent frequency coverage of these observations allows us to define the spectral parameters at the two epochs with high accuracy. We fitted the flare data at these epochs with a model spectrum corresponding to self-absorbed synchrotron emission from a uniform, face-on slab. The optically thin spectrum can be fitted by a power law of spectral index $\alpha \approx -1.2$, with no evidence of a break at near-IR frequencies. This contrasts with the properties of the quiescent spectrum, which has $\alpha \approx -0.7$ and exhibits a steepening above about 10^{14} GHz. It is apparent that the flaring spectrum evolved between the two epochs, with the peak flux density S_m increasing from 14 ± 1 to 26 ± 1 Jy and the turnover frequency ν_m decreasing from 370 ± 30 to 300 ± 30 GHz. The millimeter-wave data at the later epochs show that the flux density at the turnover, S_m, subsequently remained at about the same

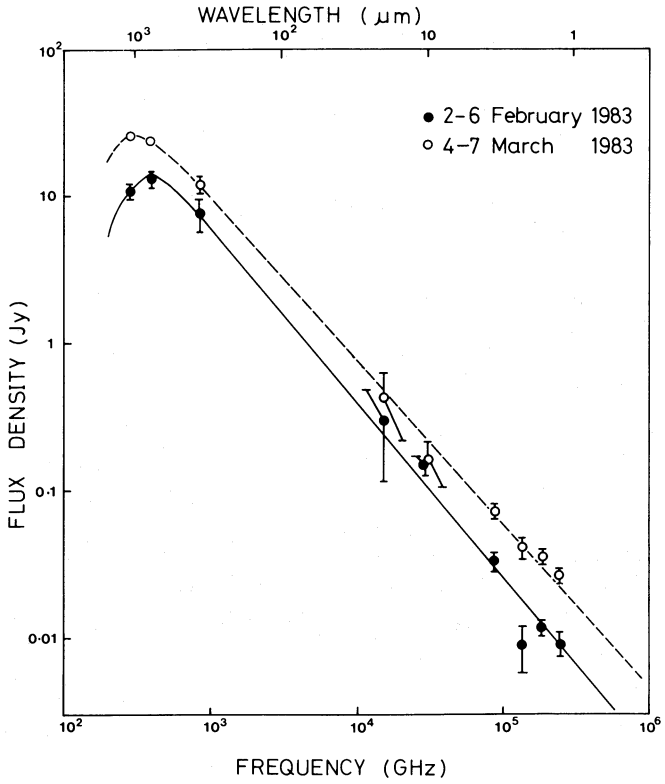

FIG. 1.—Observed flare spectrum of 3C 273 at epochs 1 and 2 in early 1983. Flux densities are obtained by subtracting the "quiescent" spectrum of Clegg *et al.* (1983) from the flare data of Robson *et al.* (1983). Curves correspond to the theoretical synchrotron spectra of uniform, face-on slabs.

© American Astronomical Society • Provided by the NASA Astrophysics Data System

1985ApJ...298..114M

level as in early March, while ν_m continued to decrease with time (see Robson *et al.* 1983). In addition, near-IR measurements by Robson *et al.* show that the high-frequency flux density had essentially dropped to its quiescent level by late April.

Further information on the outburst is obtained from the 89 GHz VLBI observations reported by Backer (1984). These data indicate that the source angular size was about 0.2 milliarcseconds (mas) in April. Since the spatial frequency coverage was rather limited, it is not clear whether this "size" pertains to the separation of components or to the angular extent of one dominant component. In either case, this result (plus Backer's finding that a previous flaring component must have either expanded or separated from the core at a superluminal speed) implies that the highly variable component expands or moves with an apparent velocity exceeding $3h^{-1}c$, where h is Hubble's constant in units of 100 km s^{-1} Mpc^{-1}.

III. INTERPRETATION OF THE EARLY 1983 FLARE OF 3C 273

a) General Considerations

Since we have well-determined flaring spectra for only two epochs, we cannot specify uniquely the physical evolution of the flaring component of 3C 273 in early 1983. Nevertheless, the information contained in these two spectra, plus the later limited frequency range data, is sufficient for us to determine the salient phenomenological properties of the outburst.

One result which is immediately apparent is that the optically thin spectral index of the flaring component (see Fig. 1) is an additive factor of about 0.5 steeper than that of the quiescent emission (Clegg *et al.* 1983). This is expected if the relativistic electrons responsible for the flare are continuously injected with the same energy distribution as for the quiescent emission and subsequently suffer significant energy losses to synchrotron radiation or Compton scattering (Kardashev 1962).

Further clues to the physical nature of the outburst come from the change in the spectrum of the flaring component from 1983 February 2–6 (epoch 1) to 1983 March 4—7 (epoch 2). The peak flux density at optically thin frequencies rose by a factor of 1.86 ± 0.15 between these two epochs, while the turnover frequency decreased by a factor of 1.23 ± 0.15. That the turnover frequency should decrease while the flux density increases severely constrains any model for the flare, since, as we now show, both quantities depend on the physical parameters in a similar manner. We adopt an electron energy distribution given by

$$N(E) = KE^{-s},$$

with $s = 1 - 2\alpha$. The value $s = 3.4$ is used for the flaring component, and $s = 2.4$ for the quiescent component. We also adopt a magnetic field $\boldsymbol{B}$ (assumed uniform in strength, nearly random in direction); circular symmetry with dimension R perpendicular to the line of sight and x along the line of sight; and a Doppler factor δ (the superluminal motion of the radio knots indicates an average value $\delta \approx 6h^{-1}$ for the most likely angle of ejection; Unwin *et al.* 1985). Standard incoherent synchrotron formulas (e.g., Pacholczyk 1970) yield, for the optically thin flux density, turnover frequency, and maximum flux density,

$$\begin{aligned} S_\nu &\propto KB^{(s+1)/2}R^2x\delta^{(s+3)/2}\nu^{-(s-1)/2} \\ &\propto KB^{2.2}R^2x\delta^{3.2}\nu^{-1.2} \qquad (s = 3.4), \end{aligned} \tag{1}$$

$$\begin{aligned} \nu_m &\propto (KB^{(s+2)/2}x\delta^{(s+2)/2})^{2/(s+4)} \\ &\propto K^{0.27}B^{0.73}x^{0.27}\delta^{0.73} \qquad (s = 3.4), \end{aligned} \tag{2}$$

and

$$\begin{aligned} S_m \equiv S_\nu(\nu_m) &\propto (K^5B^{2s+3}x^5\delta^{3s+7})^{1/(s+4)}R^2 \\ &\propto K^{0.68}B^{1.3}x^{0.68}\delta^{2.3}R^2 \qquad (s = 3.4). \end{aligned} \tag{3}$$

We shall assume for simplicity that δ is constant; it is clear that changes in δ alone cannot account for the increase in S_m while ν_m decreases. The use of these equations implicitly assumes that light travel time effects do not affect the proportionalities. The major qualitative differences in the dependence of S_m and ν_m on the physical parameters are the weaker dependence of ν_m on all parameters and the extra R^2 factor in the expression for S_m. The latter indicates that it is *expansion of the flaring component* which causes S_m to increase while ν_m decreases between epochs 1 and 2. Although it is mathematically possible for a stationary or contracting source to simulate the observed behavior, this would require very strange and drastic changes in the parameters B, K, and/or x.

We find it useful for the purpose of constructing models to express the variation of the peak flux density S_m as a power law of the turnover frequency ν_m. This is not necessarily a correct formulation, but it should be accurate at least over limited periods of time. For the early evolution of the flare, we find for the peak flux density

$$S_m \propto \nu_m^{-y}, \qquad y = 3.0^{+4.4}_{-1.4} \qquad \text{(epochs 1–2)}. \tag{4}$$

(We note that it is the lower bound to y which most constrains possible models.) Beyond epoch 2, the peak flux density remained roughly constant, i.e.,

$$S_m \sim \text{const.} \propto \nu_m^0 \qquad \text{(later epochs)}. \tag{5}$$

Although the data are certainly not sufficient to specify uniquely how the source evolved physically during the flare, we consider two idealized models which are cable of describing the observed behavior of the outburst.

In Appendix A we determine the evolution of a uniform, expanding source, allowing for variable injection of relativistic electrons and magnetic field and including synchrotron, Compton, and expansion losses. There we show that a model based upon a uniform expanding source can reproduce the observed behavior of 3C 273 if the injection of relativistic electrons is allowed to vary with

© American Astronomical Society • Provided by the NASA Astrophysics Data System

1985ApJ...298..114M

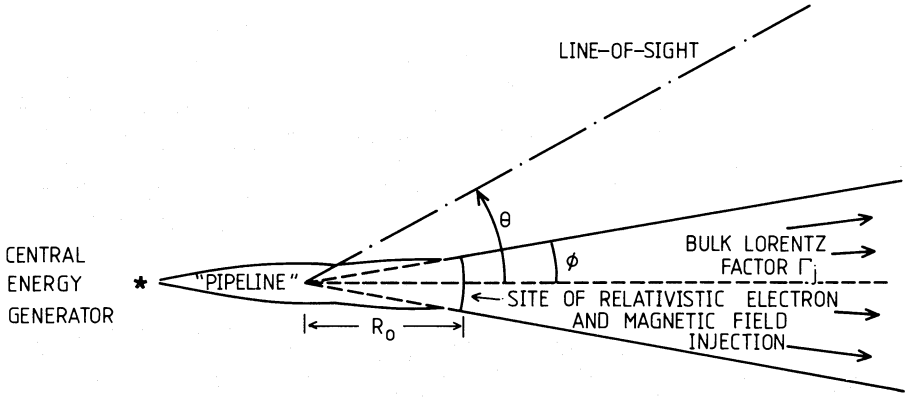

FIG. 2.—Sketch of the relativistic jet geometry discussed in the text. The nature of the "pipeline" from the central energy generator to the jet is unknown and may not exist. Not drawn to scale.

radius in a rather ad hoc fashion. There is no obvious reason why the empirical values of the injection index Q should take on the required values both before and after epoch 2. In fact, it is extremely likely that the success of this model is derived solely from its large number of free parameters (Q, a, and D) relative to the single exponent which the model attempts to reproduce (the parameter y of expression [4]). One should therefore probably add a constraint that the combination of the parameters Q, a, and D correspond to the expectations of a reasonable physical model of the source.

b) Shock Wave in a Relativistic Jet

In view of the unsatisfactory nature of the uniform expanding source model, we now try a different approach. We adopt a physical model of the source and then determine whether the time behavior of the model is in accord with the observations. This reduces the number of free parameters but also reduces the probability that a given model will fit the data. Conversely, we can consider the model strongly supported if it does reproduce the observations satisfactorily.

The model which we choose assumes the existence of a relativistic jet directed nearly along the line of sight. Such a jet was first proposed by Blandford and Rees (1978) to account for some of the properties of compact extragalactic radio sources, especially superluminal motion and rapid variability. Further theoretical development of the observable properties of these jets is contained in papers by Blandford and Königl (1979), Marscher (1980), and Königl (1981). Each of these studies introduces complications which do not now appear necessary to explain the spectra of objects such as 3C 273. Here we adopt a simple physical model, similar to that presented by Königl (1981) and shown in Figure 2, in which the jet is conical, with constant opening half-angle ϕ and with relativistic electrons and magnetic field injected at a point which lies an axial distance R_0 from the vertex of the cone. (We note that the vertex need have no physical significance; e.g., it does not necessarily coincide with the central energy source.) The plasma injected at R_0 flows steadily outward at a relativistic speed characterized by a constant Lorentz factor Γ_j. The axis of the cone makes an angle θ to the line of sight. For simplicity, we assume that $\theta \gg \phi$, which allows us to assume a constant Doppler factor δ. This assumption is supported by the apparent lack of sources viewed directly down the beam (A. P. Marscher, in preparation). (Since we are mainly concerned with proportionalities, it is unlikely in any case that this assumption substantially affects the validity of our results.)

We follow Marscher (1980) by assuming that the jet flow is adiabatic. The energy of a relativistic electron then falls off as $R^{-2/3}$. The parameter K of the electron energy distribution is, at a distance R from the vertex of the cone, then given by

$$K = K_0(R_0/R)^{2(s+2)/3} \propto R^{-2.93} \qquad (s = 2.4)\,. \tag{6}$$

Here we have identified the jet with the bulk of the "quiescent" emission of 3C 273; hence the value $s = 2.4$. The magnetic field strength is assumed to fall off as R^{-a}. The slope of the synchrotron spectrum below the turnover frequency is then

$$\alpha_{\rm thick} = [3(2s + 3)a + 4s - 19]/[3(s + 2)a + 2(2s + 1)]$$

(Marscher 1980; Königl 1981). For $s = 2.4$, we find $\alpha_{\rm thick} = 0.56$ for $a = 1$ and $\alpha_{\rm thick} = 0.98$ for $a = 2$. Unwin *et al.* (1985) find $\alpha_{\rm thick} = 0.65 \pm 0.15$ for the "core" on their VLBI maps. If we identify the core with the unresolved narrow end of a jet, the $a = 1$, $\alpha_{\rm thick} = 0.56$ case would be consistent with the observed spectral slope. It is also possible that the "core" is a blending of the jet plus a superluminal knot, which would allow the values $a = 2$, $\alpha_{\rm thick} = 0.98$ (as well as other values of $\alpha_{\rm thick}$ steeper than 0.65) for the jet. Future, 90 GHz VLBI observations should eventually yield a more accurate dissection of the spectrum of 3C 273.

Changes in the injection rate of relativistic electrons and/or magnetic field at radius R_0 or in the bulk Lorentz factor of the flow would cause variability of the observed jet spectrum. If the injection radius R_0 remains constant, increases in the above three parameters will, in general, cause both the flux density and the turnover frequency to rise. More complicated variations, such as a change in the injection site R_0, or a decrease in bulk Lorentz factor accompanied by an increase in K and B, could, in principle, reproduce the behavior of 3C 273 between epochs 1 and 2 (decrease in ν_m during an increase in S_m), but we currently have no

© American Astronomical Society • Provided by the NASA Astrophysics Data System

1985ApJ...298..114M

physical basis for supposing that these possibilities might occur. Instead, it seems more reasonable to investigate the behavior of a necessary consequence of variations in the flow parameters: the formation of shock waves. Shocks in relativistic jets have previously been proposed to account for both the appearance of superluminal knots in compact sources (Blandford and Königl 1979; Jones 1982; Lind and Blandford 1985) and the variable polarization of BL Lacertae (Aller and Aller 1984).

Any increase in the pressure of the jet flow will result in the formation of a shock. A minor disturbance propagates as a sound wave and steepens into a shock as it encounters the pressure gradient in the jet. Jones (1982) has considered this case in the adiabatic limit, but has yet to publish the full results. Here we concentrate on the case in which the increase in the jet flow is significant enough to result in the production of at least a moderately strong shock. This can be accomplished either through a substantial increase in the pressure of the jet plasma (viz., an increase in the parameter K_0) or in the bulk velocity of the flow (Rees 1978). The strong shock limit has the advantage of having analytic solutions, but is difficult to obtain in a relativistic jet (see Appendix B). Hence, we will only use the strong shock limit as a rough guide to the properties of moderately strong shocks which are relevant to our study.

We shall assume that, as in the case of a strong shock, we can define a compression ratio η such that the number densities in front of and behind the shock front follow the law

$$\frac{n_2'}{n_j'} \equiv \eta \xrightarrow[\text{strong shock limit}]{} \frac{\hat{\gamma}_2 \Gamma_2' + 1}{\hat{\gamma}_2 - 1} \approx \frac{13\Gamma_2' + 9}{4} \tag{7}$$

(Blandford and McKee 1976), where the last approximation corresponds to $\hat{\gamma} = 13/9$. (See Appendix B for definitions of the parameters to the right of the arrow.) We will also assume that each relativistic electron gains energy by some constant factor ξ as it crosses the shock front. For an adiabatic acceleration process, $\xi = \eta^{1/3}$, which may be regarded as a lower limit. (It is not clear whether the acceleration mechanism discussed in relation to shocks in supernova remnants [Blandford 1979, and references cited therein], which requires multiple passages of particles through the shock front, operates in this case. A necessary ingredient of this mechanism is the efficient scattering of the particles off plasma waves. It has not been shown whether such plasma waves, which probably exist in the interstellar medium of our Galaxy, can be present in a relativistic jet, which has no "cold background" plasma.) The relativistic electron spectral parameter K thus maintains the same form as in expression (6), with the effective value of K_0 increasing by a factor $\eta\xi^{s-1}$. The component of the magnetic field $B_\perp$ which lies perpendicular to the jet axis and therefore parallel to the shock front, is amplified by a factor η. The field is apparently rather turbulent in the jet, with $B_\perp \sim B_\parallel$ (Jones *et al.* 1985). Hence, we expect the field in the shocked plasma to have a strength of roughly $B \approx (\eta^2 + 1)^{1/2} B_\perp$. As Blandford and Rees (1974) have pointed out, one expects the relation $B_\perp \propto R^{-1}$ to hold in a jet; hence, the field behind the shock front should also fall off as R^{-a}, with $a = 1$. In some cases it may occur that $B_\parallel \gg B_\perp$ in the jet; under this circumstance the field is not substantially amplified by the shock and $a = 2$.

Since the shock is not arbitrarily strong, we cannot use the blast-wave similarity solutions which describe how the physical parameters of the shocked plasma vary with distance behind the shock front (Blandford and McKee 1976). Rather, we approximate that the density, etc., of the shocked plasma is constant up to a distance $x_{\max}$ behind the shock front, beyond which it drops to zero (a similar approximation is made by Lind and Blandford 1985). We do not expect this to introduce significant errors in our resulting proportionalities. Because of synchrotron and Compton radiation losses, the highest energy electrons will suffer substantial decreases in energy by the time they have traveled a distance $x \ll x_{\max}$. For an electron which radiates mostly near frequency $\nu_{\rm GHz}$ GHz, synchrotron losses will limit the value of x to

$$x \approx 0.4 B^{-3/2} \nu_{\rm GHz}^{-1/2} [\delta/(1+z)]^{1/2} \beta_{\rm rel} \text{ pc} \qquad (\nu_{\rm GHz} \gtrsim \nu_*) , \tag{8}$$

where

$$\nu_* = 0.2 x_{\max,\,\rm pc}^{-2} B^{-3} [\delta/(1+z)] \beta_{\rm rel}^2 \text{ GHz} . \tag{9}$$

Here, $\nu_{\rm GHz}$, δ, and z are measured in the observer's frame, and B and x in the comoving frame of the shocked gas; $\beta_{\rm rel}$ is the velocity (in units of c) of the shock front in the frame of the shocked gas, e.g., $\beta_{\rm rel} \approx 0.1$ for $\Gamma_2 = 1.1$. Upon taking into account length contraction and differential time delays (see Lind and Blandford 1985), we find that, in the observer's frame, the effective thickness of the shock is roughly Γ_2 times that given by expression (8).

If we substitute expression (8) and the relations between K, B, and R in expressions (1), (2), and (3), we find for the optically thin flux density, turnover frequency, and maximum flux density of the shocked region, for $B^2 \gg 8\pi u_{\rm ph}$ and $\nu_{\rm GHz} \gg \nu_*$ (which we shall call the "synchrotron stage"),

$$\begin{aligned} S_\nu &\propto R^{-[4(s-1)+3a(s-2)]/6} \nu^{-s/2} \\ &\propto R^{-1.13} \nu^{-1.2} \qquad (s = 2.4, \quad a = 1) , \end{aligned} \tag{10}$$

$$\begin{aligned} \nu_m &\propto R^{-[4(s+2)+3a(s-1)]/[3(s+5)]} \\ &\propto R^{-0.98} \qquad (s = 2.4, \quad a = 1) , \end{aligned} \tag{11}$$

and

$$\begin{aligned} S_m &\propto \nu_m^{[(2s-5)(2+3a)]/[4(s+2)+3a(s-1)]} \\ &\propto \nu_m^{-0.05} \qquad (s = 2.4, \quad a = 1) . \end{aligned} \tag{12}$$

Although it is clear that expression (12) cannot describe the evolution of the 3C 273 flare between epochs 1 and 2, it does provide the required nearly constant value of S_m observed after epoch 2 (cf. relation [5]). Given this possible success, we now calculate similar expressions for the case in which Compton losses are dominant.

© American Astronomical Society • Provided by the NASA Astrophysics Data System

1985ApJ...298..114M

In order to include the effects of Compton losses, we adopt the same approximations used to derive expressions (A4)–(A10). In the case of the shock model, however, it is x rather than K which is affected by the Compton losses. Expression (8) is still valid for x if we multiply the right-hand side by $B^2/(8\pi u_{\rm ph})$; we also multiply the right-hand side of equation (9) for ν_* by $[B^2/(8\pi u_{\rm ph}]^2$. We then obtain the relations, for $8\pi u_{\rm ph} \gg B^2$ and $\nu_{\rm GHz} \gg \nu_*$ (which we shall call the "Compton stage"),

$$u_{\rm ph} \propto K(B^{3s+7}R^{s+5})^{1/8} \propto R^{-U}\,, \tag{13}$$

$$U = [(13s + 17) + 3a(3s + 7)]/24$$
$$= 3.8 \qquad (s = 2.4, \quad a = 1)\,, \tag{14}$$

$$S_\nu \propto R^{[(11-s)-a(s+1)]/8}\nu^{-s/2}$$
$$\propto R^{0.65}\nu^{-1.2} \qquad (s = 2.4, \quad a = 1)\,, \tag{15}$$

$$\nu_m \propto R^{-(a+1)/4}$$
$$\propto R^{-1/2} \qquad (a = 1)\,, \tag{16}$$

and

$$S_m \propto \nu_m^{-(11-a)/[2(a+1)]}$$
$$\propto \nu_m^{-5/2} \qquad (a = 1)\,. \tag{17}$$

We see that proportionality (17), which is independent of s, lies well within the observed relation between epochs 1 and 2 of the 3C 273 flare (see relation [4]). Also, since $u_{\rm ph}$ decreases more rapidly than B^2, we find that the importance of synchrotron losses relative to Compton losses increases with time such that the S_m-ν_m relation should evolve from that given in expression (17) to that given in expression (12) (and eventually to that given by expression [20] below).

We therefore find that the shock model is very successful in reproducing qualitatively the evolution of the early 1983 flare of 3C 273. Taking into account our comments at the beginning of this subsection, we feel that either the agreement of the shock model with the observations is a remarkable coincidence, or the shock model is a good representation of the actual physics of the flare.

We have discussed the nature of a flare caused by a shocked relativistic jet (actually, none of the proportionalities are affected by the assumption that the jet is relativistic, since we have assumed constant Doppler factor δ; however, they are derived under the premise that the x dimension lies nearly along the line of sight, as is required for relativistic beaming but not in general) during the stages when Compton and synchrotron losses determine the structure of the region of enhanced emission. During the initial stages when Compton losses dominate, the flux density rises at all frequencies, with only a small change in the turnover frequency. (The flux density will also rise at all frequencies as the shock develops; in the case of 3C 273, this stage apparently occurred before the flare was first detected.) Later, in the synchrotron loss stage, the peak flux density remains roughly constant ($s = 2.5$) or rises ($2 < s < 2.5$) or falls ($s > 2.5$) slowly with time. Once the radiative lifetime of the electrons which emit at frequency $\nu \sim \nu_m$ exceeds the time it takes to cross the density scale length of the shock (viz., $\nu > \nu_*$; cf. eq. [9]), a new stage emerges, the "adiabatic" stage. (The term "adiabatic" refers to the dominant energy losses of the electrons which radiate mainly at the observed frequency, rather than to the shock itself, which is adiabatic at all stages discussed thus far.) We expect the shock to be roughly self-similar, although this holds strictly only for a blast wave; hence $x = x_{\rm max} \propto R$. For $a = 1$, we then find

$$S_\nu \propto R^{-7(s-1)/6}\nu^{-(s-1)/2}\,, \tag{18}$$

$$\nu_m \propto R^{-(7s+8)/[3(s+4)]}\,, \tag{19}$$

and

$$S_m \propto \nu_m^{10(s-1)/(7s+8)}\,. \tag{20}$$

The exponent in proportionality (20) equals 0.45 for $s = 2$ and 0.69 for $s = 3$. Notice that it is identical with the spectral index of the undisturbed jet below the turnover given above.

IV. DISCUSSION OF THE SHOCKED JET MODEL

a) *Quantitative Model for the Compact Jet of 3C 273*

While the number of approximations which we have made renders it impossible to determine accurately all the physical parameters of the shocked jet model, it is desirable to estimate the values of certain parameters in order to determine whether the model can plausibly be applied to 3C 273. We can estimate the value of R_0 by requiring that Compton losses do not kill off the electrons which radiate in the IR before they are able to propagate a considerable distance from the injection site. This restricts the maximum observed brightness temperature of the jet to a value

$$T_m \lesssim 3 \times 10^{11}[\delta/(1 + z)]^{1.2}\,.$$

Since observations nearly always show that T_m is not much less than this limit, we can change the inequality to an approximate equation. If we integrate along the line of sight in a manner identical with that of Königl (1981), we find that this is equivalent to

$$R_0 \approx 7(\phi \sin\theta)^{-1/2}\delta^{-0.6}(1 + z)^{-1.4}D_l S_m^{1/2}\nu_m^{-0.9}\ \text{pc}\,, \tag{21}$$

© American Astronomical Society • Provided by the NASA Astrophysics Data System

1985ApJ...298..114M

where D_l (luminosity distance), S_m, and ν_m are measured in Gpc, Jy, and GHZ, respectively. Following the spectral dissection of Unwin *et al.* (1985) for the quiescent emission, which we identify with the undisturbed jet, we adopt the values $\nu_m \approx 70$ and $S_m \approx 25$. Also, $D_l = 0.47h^{-1}$. Since we require the jet to have a somewhat lower Lorentz factor than the superluminal knots (for which Unwin *et al.* 1985 obtain $\Gamma \gtrsim 7h^{-1}$), we set $\Gamma_j \approx 5h^{-1}$. The jet opening angle ϕ and inclination of the jet axis to the line of sight θ are not very well constrained. Unwin *et al.* (1985) favor $\sin\theta \lesssim 0.1$ and $\phi \gtrsim 0.01$ radians mainly on the basis of geometric constraints. Also, as noted previously, the model assumes, and the data support, $\phi \ll \theta$. Here we adopt $\sin\theta \approx 0.1$ and $\phi \approx 0.02h$ radians. We also assume that the jet magnetic field falls off as R^{-1} (i.e., $a = 1$). We then derive $\delta \approx 8h^{-1}$ for the jet.These values lead to the estimate $R_0 \approx 1.9h^{-1.4}$ pc. Also, adapting Königl's (1981) basic analysis (based on standard synchrotron theory and the assumption that the spectral turnover is caused by synchrotron self-absorption) to our specific jet model, we obtain the following estimates for the magnetic field and electron energy spectral parameter K at R_0:

$$B_0 \approx 0.2(\phi \sin\theta)^{-1/2}\delta^{-2}D_l S_m^{1/2}\nu_m^{0.5} \approx 1h^{1/2}\ \mathrm{G}\ , \tag{22}$$

$$\begin{aligned} K_0 &\sim 5\times 10^{-11}(\phi^{-1}\sin\theta)\delta^{-2.2}(1+z)^{3.2}B_0^{-2.2}R_0^{4.1}\nu_m^{3.2} \\ &\sim 5\times 10^{-6}\phi^{-2.0}\delta^{-0.3}(1+z)^{-1.4}D_l^{1.9}S_m^{1.0}\nu_m^{-1.6} \\ &\sim 4\times 10^{-5}h^{-3.6}\quad (\text{cgs units})\ . \end{aligned} \tag{23}$$

Another method of estimating B_0 is to ascribe the spectral break at $\nu_b \approx 10^{14}$ Hz in the quiescent spectrum to the effects of synchrotron losses (Königl 1981). Upon taking the gradient in B into account, we obtain

$$\begin{aligned} B_0 &\approx \{8\times 10^4[\delta/(1+z)]^{1/2}\Gamma_j\nu_b^{-1/2}R_0^{-1}\}^{2/3} \\ &\approx 0.15h^{-0.1}\ \mathrm{G}\ , \end{aligned} \tag{22'}$$

where ν_b is measured in Hz. Although this estimate differs by almost an order of magnitude from that given in expression (22), the discrepancy is within the uncertainty of the analysis. We split the difference logarithmically to settle on the estimate $B_0 \sim 0.4$ G, with an uncertainty of a factor of about 3. The energy density in relativistic electrons at R_0 is roughly $2.5K_0E_{\min}^{-0.4} \sim 10^{-2}(E_{\min}/10^{-5}$ ergs$)^{-0.4}h^{-3.6}$ ergs cm^{-3}. We compare this with the energy density in magnetic field $B_0^2/8\pi \sim 6\times 10^{-3}$ ergs cm^{-3}. We therefore find that the plasma is near equipartition between the relativistic electrons and the magnetic field, although we again stress that the uncertainties are large. Nevertheless, it is interesting that the relativistic electrons do not appear to dominate the energy density overwhelmingly, as is often the case for individual (noncore) components in other similar sources (e.g., Kellermann and Pauliny-Toth 1981). We also note with interest that the energy density and characteristic length scale R_0 are of the same order as the pressure and radius of the broad emission line region, $\sim 10^{-2}$ ergs cm^{-3} and 1–10 pc, respectively, so that it is quite possible that the same hot, gaseous medium confines both the inner portion of the jet and the emission-line clouds (see also Rees 1984 for further discussion of this point). The total energy input required to maintain the energy density of the jet is $\pi(\phi R)^2\Gamma_j c$ times the energy density, or $6\times 10^{43}(E_{\min}/10^{-5}$ ergs$)^{-0.4}h^{-5.4}$ ergs s^{-1}. Even for $h = 0.5$, this is $3\times 10^{45}(E_{\min}/10^{-5}$ ergs$)^{-0.4}$ ergs s^{-1}, less than one-third the optical luminosity of 3C 273.

The characteristic observed angular size of a shock in the jet is roughly

$$2\phi R(1+z)^2/D_l \sim 0.04h^{0.6}(R/R_0)\ \mathrm{mas}\ , \tag{24}$$

if we assume that the shock extends across the entire width of the jet. In order to determine the value of R for the shock model at a particular epoch of the 3C 273 flare, we use relation (16) and the observed ratio of turnover frequencies for epochs 1 and 2, $\nu_m(\text{epoch 1})/\nu_m(\text{epoch 2}) = 1.23 \pm 0.25$, and note that expression (17) corresponds to the middle of the allowed range (cf. proportionality [4]). We then find $R_2 \approx 1.5R_1$, where the subscripts refer to epochs. Since we know the time between these epochs, $(t_2 - t_1) \approx 30$ days, we can use the formula

$$R_2 - R_1 = \beta_s c(t_2 - t_1)(1+z)^{-1}(1-\beta_s\cos\theta)^{-1} \approx \Gamma_s\delta_s c(t_2 - t_1)(1+z)^{-1}$$

(Rees 1967). We combine these expressions to derive $R_1 \approx 1.8h^{-1}$ pc and $R_2 \approx 2.7h^{-1}$ pc, for $\Gamma_s \approx 7h^{-1}$ and $\sin\theta \approx 0.1$ (which gives $\delta_s \approx 9$). We then find that $R \sim R_0$ near the onset of the flare. This implies that the shock was formed in response to a significant increase in the pressure of the jet plasma or a sudden increase in the Lorentz factor of the flow. A minor perturbation in the pressure or a slower buildup of flow velocity would cause the shock to form further downstream (Jones 1982; Rees 1978).

The observed angular extent of the shock at epoch 2 is found from expression (24), given $(R_2/R_0) \approx 1.5h^{0.4}$, to be $\sim 0.06h$ mas. If we insert this and the other parameters relevant to epoch 2 into standard synchrotron formulas (e.g., Jones, O'Dell, and Stein 1974), we derive the estimated values $B_s \sim 10h^3$ G and $K_s \sim 7\times 10^{-7}[R/x(\nu_m)]h^{-3.4}$ (cgs units) for the shock component. Since our model requires that synchrotron losses begin to dominate at epoch 2, we use expression (8) to estimate $x(\nu_m) \sim 2\times 10^{-4}h^{-5}$ pc, so we find $K_s \sim 5\times 10^{-3}h^{0.6}$ in cgs units. The value of the shock compression ratio η required by these values of B and K_s therefore ranges from about 3 to 20 for h between 1 and 0.5. This agrees satisfactorily with the expected limit $\eta \lesssim 6$ (see expression [7]).

We therefore conclude that, within the limits of our approximate analysis, a numerically consistent relativistic jet model can be created to explain both the quiescent emission and the early 1983 flare of 3C 273. The magnetic field at the base of the jet lies between 0.15 and 1 G, and the relativistic electrons are not too far from energy equipartition with the magnetic field (although it is still possible that the electrons dominate by one or two orders of magnitude, especially if $h \approx 0.5$). The relativistic electrons are accelerated or injected about 2 pc from the apex of the jet cone, which may itself lie a considerable distance from the central energy generator. The shocked region should have characteristic dimensions $\phi R \sim 0.04$ pc radius by $x \approx x_{\mathrm{obs}}/\Gamma_2 \sim 2\times 10^{-4}h^{-5}(\nu/\nu_m)^{-1/2}$

© American Astronomical Society • Provided by the NASA Astrophysics Data System

1985ApJ...298..114M

pc thickness. (Projection effects cause x_{obs} to appear foreshortened by a factor $\sin\theta \approx 0.1$, so that the actual measured value $x_{meas} \approx x$.) The minimum time scale of variations from such a region can be as short as

$$(\Delta t)_{var} \sim (x/c)[(1+z)/\delta] \sim 0.03h^{-4}(v/v_m)^{-1/2} \text{ days} . \quad (25)$$

This corresponds to a plane shock viewed head-on. The assumed curvature of the shock yields a time scale $\sim 0.5\phi^2 R/c$ when viewed head-on, whereas the effects of inclination yield a time scale $\sim \phi(R/c)\sin\theta$. The actual minimum variability time scale is the maximum of these three expressions. For 3C 273, the last is the greatest, which leads to $(\Delta t)_{var} \gtrsim \phi(R/c)\sin\theta \sim 4h^{-0.4}$ days. We wish to use this expression to make an important point which is nearly always overlooked in studies of time variability in quasars and active galactic nuclei: *the observation that a source varies with time scale Δt does not necessarily imply that the variable component lies within a distance $\sim c\Delta t[\delta/(1+z)]$ of the central energy source.*

b) *Limitation on the Value of s in the Shocked Jet Model*

It is important for us to point out that the shocked jet model presented in the previous section is subject to the restriction that the exponent of the relativistic electron energy distribution s must be greater than 2. The spectral index of the observed emission is restricted to $\alpha = -(s-1)/2 < -0.5$ below the break frequency (in the quiescent as well as the variable component) and $\alpha = -s/2 < -1$ above the break frequency. For $s < 2$, the highest energy electrons supply the bulk of the energy density and pressure. Therefore, as they cool from radiation losses, the pressure decreases substantially. The shock would then be radiative, hence the dynamics would be altered considerably (Blandford and McKee 1976). Such a shock would not propagate far down the jet unless it were extremely strong initially. Our model assumes that the shock is nonradiative.

We hasten to point out that of the highly variable sources observed in the far-IR thus far, all have IR spectral indices steeper than -0.5 (Gear *et al.* 1985*a*, *b*), in keeping with the requirement of our model.

c) *Application of the Shocked Jet Model to Variable Radio Sources in General*

Since we have successfully applied the shock model to 3C 273, it seems natural to expect that it can also be used to explain variable extragalactic radio sources in general. The statistical and individual patterns of variability in extragalactic objects have been explored by many authors, with Aller and Aller (1985), Altschuler and Wardle (1976, 1977), Andrew *et al.* (1978), Epstein *et al.* (1982), and O'Dea, Dent, and Balonek (1984) discussing the results of many years of observation at a number of wavelengths. Although it is beyond the scope of this paper to discuss whether our model can explain every facet of variable source behavior, it is important to ascertain whether it can reproduce the trends observed in the majority of sources.

As is discussed by Altschuler and Wardle (1977), Andrew *et al.* (1978), Epstein *et al.* (1982), and O'Dea, Dent, and Balonek (1984), the general behavior of source variability can be described by the following pattern: (1) the outbursts tend either to occur nearly simultaneously at centimeter and millimeter wavelengths or to appear first in the millimeter region, then propagate to longer wavelengths; (2) the maximum outburst flux density decreases toward longer radio wavelengths, with a mean law $S_{max}(\nu) \propto \nu^{\zeta}$, where $\langle\zeta\rangle \approx 0.4 \pm 0.2$; (3) the spectral turnover of the flaring component is considerably broader than one would expect from a uniform synchrotron source; (4) the peak flux densities often occur nearly simultaneously or with short time delays at centimeter wavelengths; (5) some events are observed which are best described as "quenchings" of previously stable flux densities (Epstein *et al.* 1982); and (6) several sources observed in the submillimeter and IR regions by Gear *et al.* (1985*b*) show a transition from an initially flat (optically thick) to a steep (optically thin) submillimeter spectrum. This evolution is typically associated with a decrease in flux density and steepening of the IR spectrum, but with very little change in the submillimeter flux density; this matches the behavior observed during the second stage of the early 1983 flare of 3C 273.

During the adiabatic stage (and also during the later part of the Compton/synchrotron loss stage) the value of x in the observer's frame, x_{obs}, is large enough that the shocked region encompasses a sizable fraction of the jet, viz., the inner radius of the shock R_{in} is considerably less than the outer radius R, by perhaps a few tens of percent. The shocked region then appears somewhat inhomogeneous to the observer, in that the values of B and K are considerably less at R than they are at R_{in}, since the material at R_{in} was shocked closer to the vertex of the cone. These inhomogeneities broaden the spectral turnover of the shocked region compared with a uniform source, as is required by the observations. For the extreme case $(R - R_{in}) \rightarrow R$ the spectral index below the turnover becomes the same as that of the jet,

$$S_\nu \propto \nu^{10(s-1)/(7s+8)} , \quad (26)$$

again for $a = 1$. Since this is identical with the S_m versus ν_m law, the flux density at $\nu < \nu_m$ would remain constant during the adiabatic stage until $\nu_m < \nu$, after which it would fall. This behavior is similar to the quenching observed in some sources by Epstein *et al.* (1982).

Expression (20) shows that the dependence of peak flux density on frequency should follow the law $S_m \propto \nu_m^{\zeta}$, with ζ between about 0.5 and 0.7 for typical values of s, during the adiabatic phase. A flatter dependence, $\zeta = 0$–0.4, should prevail during the synchrotron loss stage. Although these values of ζ are not exactly equal to the observed value of 0.4, they are close enough for us to be encouraged that a more detailed calculation, which takes into account the various complications, might yield a value of ζ closer to that obtained empirically.

If the shock is still intact by the point where $E_b = E_{min}$ in the jet, $s \rightarrow s+1$, and for $s > 2$ the shock will become radiative. Such a shock would be thermally unstable and collapse to a thin shell, essentially coasting at whatever bulk Lorentz factor it had at the point when it became radiative. The flux density would then rise because of the compression, as would the turnover frequency, although ν_m is unlikely to extend to extremely high radio frequencies. After the compression ceased (stopped by proton or magnetic pressure), the component would behave in a manner similar to that of a uniform source expanding in two dimensions (see Appendix A). It is also possible for the shock to encounter inhomogeneities in the jet or previous, slower shocks. This would

© American Astronomical Society • Provided by the NASA Astrophysics Data System

1985ApJ...298..114M

produce a flare on top of a flare, or cause a faded shock component to become rejuvenated. Both these possibilities could apply to the problem of low-frequency variability, which requires outbursts with ν_m in the 0.1–1 GHz range (see also Marscher 1982; Aller and Aller 1982).

d) Application to Superluminal Motion of Radio Components

One of the most striking properties of 3C 273 is the apparent superluminal motion of its compact radio components. Our model has been designed in part to explain the superluminal knots as shocked regions in a relativistic jet (see also Rees 1978; Blandford and Königl 1979; Jones 1982). We now delineate the characteristics of these knots which can be compared with current and future observations.

When the knots are first resolved using VLBI at centimetric wavelengths, they should be in the synchrotron loss or adiabatic stage. In the adiabatic stage, their flux density and turnover frequency should decrease with time, and the components should expand in all directions, maintaining roughly the same shape. The brightness centroid therefore should appear to move with an apparent velocity $\sim\Gamma_s(1+z)^{-1}c$. The value of Γ_s should slowly decrease with time to the asymptotic value $\Gamma_s \rightarrow \Gamma_j$. Since the initial value of Γ_s is not overwhelmingly greater than Γ_j, this deceleration is only noticeable over a wide range of distances along the jet R. Since a typical component is observed only over a factor ~ 2 in R before it fades below the detectable level at any given frequency, the deceleration is not easy to observe. In fact, unless the original disturbance which gave rise to the shock is very short-lived, the shock will be "driven" at a nearly constant Lorentz factor for a certain time before beginning to decelerate (see Blandford and McKee 1976). During the synchrotron loss stage, identified by a weak dependence of S_m on ν_m, the front edge of the shock should appear to move almost uniformly (again, with a slow deceleration), while the effective shock thickness should increase with time. Hence, the trailing edge of the shock should appear to move more slowly than the leading edge. The brightness centroid therefore should also appear to move more slowly than the leading edge. During the transition from the synchrotron loss to the adiabatic stage, the centroid should thus appear to accelerate to the Lorentz factor of the leading edge. A superluminal acceleration in the quasar 3C 345 has been observed at 1.3 cm by Moore, Readhead, and Bååth (1983). We predict that future incidents of such acceleration will be observed during a change in the S_m-ν_m relation as the transition from the synchrotron loss to the adiabatic stage occurs.

Since the compression ratio of the shock increases with the shock Lorentz factor, we expect a relation between Γ_s (as indicated by the apparent superluminal velocity) and the flux density variations. The faster shock components should in general have somewhat higher flux densities at a given separation from the core (jet) component, and should persist in the synchrotron loss stage out to a larger value of R. Quantitatively, for the $a = 1$ case, we find that the point at which the Compton loss to synchrotron loss transition occurs, R_t, and the peak flux density and turnover frequency at this point, are related to the values of B, K, and δ in the shock by

$$(R_t/R_0) \propto K_s(R_0)^{12/(11s-5)} B_s(R_0)^{9(s-3)/[2(11s-5)]}$$
$$\propto K_s(R_0)^{0.56} B_s(R_0)^{-0.13} \qquad (s = 2.4)\,, \tag{27}$$

$$S_{m,t} \propto K_s(R_0)^{15/(11s-5)} B_s(R_0)^{7(2s-5)/[2(11s-5)]} \delta_s(R_0)^{(3s+10)/(s+5)}$$
$$\propto K_s(R_0)^{0.70} B_s(R_0)^{-0.03} \delta_s(R_0)^{2.3} \qquad (s = 2.4)\,, \tag{28}$$

and

$$\nu_{m,t} \propto K_s(R_0)^{-6/(11s-5)} B_s(R_0)^{(s+11)/[2(11s-5)]} \delta_s(R_0)^{(s+3)/(s+5)}$$
$$\propto K_s(R_0)^{-0.28} B_s(R_0)^{0.31} \delta_s(R_0)^{0.73} \qquad (s = 2.4)\,. \tag{29}$$

(Actually, in keeping with our previous notation, we should use δ_2, the Doppler factor of the postshock gas, instead of δ_s. However, δ_2 is less than $\sim 10\%$ smaller than δ_s, so the difference is insignificant.) We therefore see that the effect of variable shock strength on the turnover frequency is quite small. Even the peak flux density should only change by a few tens of percent from one shock to the next except in the (probably rare) case of a major disturbance of the jet flow. This, plus the weak dependence of the peak flux density on frequency during the synchrotron loss stage, causes the total radio-to-millimeter region of the spectrum to appear quite flat owing to the superposition of several similar components at different phases of evolution.

The minimum Lorentz factor of a superluminal component corresponds to the Lorentz factor of the undisturbed jet flow. In general, the components should have Lorentz factors which exceed this by at least a few tens of percent. Only extremely energetic disturbances of the jet flow should yield shock Lorentz factors exceeding that of the jet by a factor of 2 or more. The shock model predicts that the shock will eventually decelerate to the Lorentz factor of the undisturbed jet (unless it becomes radiative). We therefore predict that well-separated components should have somewhat slower superluminal velocities than the inner components.

The optically thin spectral index of a superluminal component should flatten to $-(s-1)/2$ as the component enters the adiabatic phase, except in the extreme case where the break frequency of the jet is below the turnover at this point. For 3C 273, $\nu_b(\text{jet}) \approx 10^{14}(R/R_0)^{-7/3}$ Hz, hence the break frequency reaches radio frequencies only for $R > R_b \sim 10^2 R_0$. Other sources may have considerably lower values of ν_b(jet), in which case the optically thin spectral index should steepen to $-s/2$ beyond R_b. If the source is still in the Compton loss or synchrotron loss stage when $R = R_b$, the observed spectral index will become $-(s+1)/2$ (or, equivalently, the effective value of s will steepen by 1).

The shock wave compresses the magnetic field component perpendicular to the jet axis. The linear polarization position angle (electric field vector) of a shocked region should therefore appear aligned along the axis of the jet for most geometries of the jet field (as long as $\theta \gg \phi$). However, complications such as postshock turbulence or shock geometries different from that considered here (cf. Lind and Blandford 1985) could yield a different polarization position angle. It is also possible for the jet magnetic field to lie predominantly parallel to the jet axis. In this case the field would be essentially unamplified by the shock, and the polarization position angle for both the shock and the core (which might have low polarization owing to Faraday depolarization caused by the

© American Astronomical Society • Provided by the NASA Astrophysics Data System

1985ApJ...298..114M

high density of relativistic electrons in the jet) would lie perpendicular to the jet axis. This latter case corresponds to $a = 2$; hence the development of the flare would differ in detail from the $a = 1$ case which we have found to correspond to 3C 273.

e) Compton X-Ray Emission

An important by-product of a shocked region in a relativistic jet is variable self-Compton X-ray and γ-ray emission. Our analysis is too approximate to calculate accurately the expected Compton spectrum, which is quite sensitive to uncertainties in the physical parameters. We can only state that the importance of Compton losses during the initial stages of the flare indicates that Compton scattering may produce most of the observed X-rays and γ-rays. We can also discuss some of the qualitative features of the Compton X-ray emission, which may correspond to the observed X-ray emission in many sources.

Since the Compton losses (and therefore the Compton luminosity) fall off sharply with time during the Compton-loss stage (see expressions [26] and [27]), it is evident that the Compton-scattered X-ray flare should already be in the declining phase by the time the outburst is first detected in the submillimeter region. In fact, the peak of the X-ray emission should correspond to the point when the shock becomes fully developed. We therefore predict that Compton X-ray flares should precede millimeter-to-submillimeter flares by about the typical time scale at the latter wavelength regime, ~ 1 month in the case of 3C 273. Unwin *et al.* (1985) report that an X-ray flare observed by Halpern (1982) preceded a dramatic increase in the 2.8 cm core brightness of 3C 273 by > 30 days. Since any radio outburst is delayed by several months relative to the submillimeter wavelengths according to our model, it is possible that the two events were connected. More frequent X-ray and submillimeter monitoring should help to determine whether there is a direct submillimeter–X-ray correlation of variability.

We again stress that the minimum time scale of variability of shocked jet regions in sources such as 3C 273 can be quite short (~ 1 day; cf. expression [25] and the discussion which follows), despite the fact that the regions can be removed by $\gtrsim 1$ pc from the central energy source. The minimum observed X-ray variability time scale of 3C 273 is indeed ~ 1 day (Zamorani, Giommi, Maccacaro, and Tananbaum 1984).

An apparent difficulty in ascribing the variable 3C 273 X-ray emission to self-Compton scattering from a shocked jet lies in the spectral index of the soft X-rays, $\alpha_x = -0.4$ to -0.5 (Worrall *et al.* 1979; Halpern 1982; Petre *et al*, 1984), whereas the naively expected value is $\alpha_x \approx -0.7$, the same as for the optically thin synchrotron emission from the jet (e.g., Jones, O'Dell, and Stein 1974). It is possible for α_x to be considerably flatter than -0.7 if the X-ray frequency (from 10^{17} to 5×10^{18} Hz) lies just above the Compton scattered turnover frequency,

$$\nu_{xm} \sim [E'_{\min}/(mc^2)]^2 \nu'_m \delta_s^{(s+2)/(s+4)}(1+z)^{-1} , \tag{30}$$

where $E'_{\min}$ and ν'_m are measured in the reference frame of the shocked jet flow. For an electron on the axis of the jet, the formula for the turnover frequency ν'_m is the same as that in the observer's frame ν_m (expression [1]), with $z = 0$. $\delta = 1$, and $x = \phi R$. We therefore find

$$\nu'_m \approx (1+z)\delta^{-(s+2)/(s+4)}[\phi R/x(\nu_m)]\nu_m , \tag{31}$$

and

$$\nu_{xm} \sim [E'_{\min}/(mc^2)]^2[\phi R/x(\nu_m)]\nu_m . \tag{32}$$

During the earliest phases of the flare, when the X-ray emission should have been most pronounced, $R \approx R_0 \approx 1.9h^{-1.4}$ pc, and $x \ll R$. Recall that we obtained $x(\nu_m) \sim 2 \times 10^{-4}h^{-5}$ pc at epoch 2, when $R \approx 1.5R_0$. During the Compton loss stage $x \propto u_{\rm ph}^{-1} \propto R^{3.8}$. Hence, $x(\nu_m) \sim 4 \times 10^{-5}h^{-5}$ pc and $\phi R \approx 0.04$ pc when $R \approx R_0$. We then obtain $\nu_{xm} \sim 5 \times 10^{16}(E'_{\min}/10^{-5}\ \text{ergs})^2 h^5$ Hz at R_0. The lack of Faraday depolarization in a sample of variable radio sources argues for $E'_{\min} \sim 10^{-5}$–10^{-4} ergs in the shocked regions (Jones and O'Dell 1977; Wardle 1977). We therefore estimate $\nu_{xm} \sim 10^{15}$–10^{18} Hz. The Compton scattered spectral peak is very broad compared with that of the synchrotron emission, hence the asymptotic X-ray spectral index $\alpha_x \approx -0.7$ is attained only for $\nu \gg \nu_{xm}$. A spectral $\alpha_x = -0.4$ to -0.5 can therefore be obtained at soft X-ray energies, with $\alpha_x \approx -0.7$ at hard X-ray energies. Indeed, Primini *et al.* (1979) find $\alpha_x \approx -0.7$ for 3C 273 between 20 and 200 keV. Since $E_{\min}$ should decrease and x increase as the flare develops, we predict that the soft X-ray spectral index should prove to be variable (although not strongly so) during any given event, with α_x becoming steeper with time. Also, α_x can vary somewhat from event to event, since $E'_{\min}$ most likely depends on the shock compression ratio.

f) Shortcomings and Future Work

The shocked jet model which we have presented above incorporates a number of approximations and idealizations, which we now discuss. We have chosen a simple structure behind the shock—the density remains at its value just behind the shock front, then falls off abruptly at distance $x_{\max}$ from the shock front. We have treated the acceleration of electrons by the shock in a very simplistic manner, assuming that they gain energy by some constant factor ξ. We have assumed that the jet opening angle ϕ is very much less than θ, the inclination of the jet axis to the line of sight. While this appears to hold for 3C 273, it may not hold for some other sources, in which case there would be a differential Doppler factor across the jet. We have also ignored the effects of the shock on the undisturbed jet emission, identified as the core on VLBI maps. The presence of a shock imposes on the jet an outer boundary, which decreases the frequency range over which the relatively flat spectral slope $\alpha_{\rm thick}$ pertains; the spectral index then becomes $-5/2$ below some frequency (which decreases with time) which does not lie too far below ν_m (see Königl 1981). This complicates the detailed development of the flux density outburst at $\nu < \nu_m$(jet). At times when $x_{\rm obs}$ is not greatly less than R, time delays between the front and back part of the source complicate our derived expression for ν_m versus R. We have assumed that the characteristic thickness of the shock $x_{\max}$ is proportional to R, which is strictly true only for the self-similar structures of blast waves.

© American Astronomical Society • Provided by the NASA Astrophysics Data System

1985ApJ...298..114M

An aspect of jets which we have ignored is the bending observed in many compact jets (Readhead *et al.* 1978; Biretta *et al.* 1983). Even though the intrinsic bending is probably small and amplified by projection effects, the Doppler factor δ is somewhat affected by it. As Biretta *et al.* (1983) have pointed out, jet curvature is another possible explanation for the apparent "superluminal acceleration" observed in 3C 345. The idealized jet model used here assumes a constant value of δ, which may not hold for many jets.

Because of the above shortcomings, our numerical discussions, and in some cases our proportionalities, have usually been very approximate. We are therefore in the process of calculating more realistic models. This should serve to redefine our theory, although it is not at present possible to improve the theory of particle acceleration in a relativistic shock or to include in general the effects of curved jets (since the true curvature is likely to differ from one source to the next).

V. SUMMARY

We find that the early 1983 flare of 3C 273 observed by Robson *et al.* (1983) was characterized by a spectral evolution which provides severe constraints on possible models for the outburst. (1) In general, the emitting volume must have expanded throughout the flare. (2) A uniform, expanding source model can be made consistent with the observations only if the relativistic electron distribution is allowed to develop in a rather arbitrary fashion. (3) We favor a model in which the flare arises as disturbances in the flow of an adiabatic, conical jet cause a shock wave to propagate along the jet. (4) The high-frequency emission from such a jet will be steepened by radiative energy losses, as observed. The relativistic electrons suffer first Compton losses, then synchrotron losses as the flare develops. During a later, "adiabatic," stage, radiative losses become relatively unimportant. (5) The first two stages are characterized by a rapid increase in the flux density in the millimeter-to IR region, followed by an evolution of the spectral maximum to lower frequencies with relatively constant peak flux density. This matches quite closely the observed behavior of the early 1983 flare in 3C 273. The adiabatic stage is characterized by the decay of the flux density. (6) The model naturally explains the superluminal motion observed in sources such as 3C 273, as well as the flatness of the overall radio-to-millimeter region spectra of most compact sources—the so-called cosmic conspiracy (e.g., Cotton *et al.* 1980).

The model also produces several observationally testable predictions. (1) X-ray flares in 3C 273 should precede flares in the submillimeter-to-IR region by ~ 1 month and those in the radio region by several months. Other sources should exhibit similar delays, although the characteristic time scales will vary. (2) The optically thin spectral index cannot be flatter than -0.5 in either the flaring or the quiescent component, nor can it be flatter than -1 above the break frequency. (3) Monitoring of the evolution of an individual flaring region from submillimeter through centimeter wavelengths should reveal three distinct phases, each with its own characteristic S_m-ν_m law. (4) Superluminal accelerations should occur during the transition from the synchrotron to the adiabatic stage. This should coincide with a change in the relationship between S_m and ν_m.

In order to test these predictions, one must execute multiwavelength monitoring programs over time scales of years. The best spectral region to monitor for flares is at X-ray energies; any events should then be followed up in the IR-to-millimeter and radio regions, respectively. Further, more accurate numerical development of the shocked jet model will also enable more detailed comparison of the theory with observations.

We thank Drs. T. W. Jones, S. C. Unwin, P. E. Clegg, and E. I. Robson and Mr. J. Biretta for valuable discussions. A. P. M. was supported in part by the National Science Foundation, under grant AST-8315556. W. K. G. was supported by an SERC Studentship and Postdoctoral Research Assistantship.

APPENDIX A

EXPANDING, UNIFORM SOURCE MODELS

We generalize the "standard" expanding source model (van der Laan 1966; Pauliny-Toth and Kellermann 1966) by allowing the source to expand in D dimensions. In this way, we can consider homologous expansion ($D = 3$), as well as expansion perpendicular ($D = 2$) or parallel ($D = 1$) to a symmetry axis. For simplicity, we consider only a constant expansion velocity, since the time coverage of the observations is too limited to reveal any acceleration or deceleration. It is convenient to express K and B as power laws in radius R:

$$K = K_0(R/R_0)^k/\text{volume} \propto R^k/(R^2 x) ,$$

$$B = B_0(R_0/R)^a \propto R^{-a} .$$

Formulas (2) and (3) then give

$$\nu_m \propto R^{2[k-2-(s+2)a/2]/(s+4)}$$

$$\propto R^{0.27[k-2-2.7a]} \qquad (s = 3.4) ,$$

$$S_m \propto R^{[5(k-2)+2(s+4)-(2s+3)a]/(s+4)}$$

$$\propto \nu_m^{[(2s+3)a-2(s-1)-5k]/[(s+2)a-2(k-2)]}$$

$$\propto \nu_m^{[9.8a-4.8-5k]/[5.4a-2(k-2)]} .$$

© American Astronomical Society • Provided by the NASA Astrophysics Data System

1985ApJ...298..114M

Comparing these expressions with relation (4), we find

$$k \approx (2.4 \pm 0.2)a + 0.6^{+0.7}_{-0.3} \qquad \text{(epochs 1–2)} .$$

We therefore find that the parameter k is rather tightly constrained for a given choice of a in spite of the wide range of allowed values of y (see relation [4]). If the magnetic field is "frozen in" ($a = 2$), we obtain the rather extreme value $k \approx 5.4$. If, on the other hand, there is continuous injection of magnetic field energy, at a rate which is proportional to R^b (i.e., $d[B^2(\text{volume})]/dR \propto R^b$), we obtain $a = (D - b - 1)/2$. For the constant injection ($b = 0$), homologous expansion ($D = 3$) case, $a = 1$ (cf. Pacini and Salvati 1973), which would require $k \approx 3$.

It is straightforward to generalize the formulas given by Kardashev (1962) for the case of continuous injection of relativistic electrons, to take into account variable injection rates of both particles and field (see also Peterson and Dent 1973; Reynolds and Chevalier 1984). We adopt an injection of relativistic electrons of the form $q_0(R/R_0)^Q E^{-s'}$ electrons s^{-1} ergs^{-1}, and assume that these electrons are uniformly distributed throughout the expanding volume. For the case in which only synchrotron and expansion losses are important, we find

$$N(E, R) \propto R^{1+Q}(\text{volume})^{-1}E^{-s'} \qquad (E \ll E_b) \tag{A1b}$$

$$\propto R^{2a+Q}(\text{volume})^{-1}E^{-(s'+1)} \qquad (E \gg E_b) . \tag{A1b}$$

Here E_b is a "break energy" above which the energy distribution steepens owing to synchrotron losses. For an isotropic pitch-angle distribution, the synchrotron losses take the form

$$\frac{dE}{dt} = -c_1 B^2 E^2 ,$$

where $c_1 = 1.58 \times 10^{-3}$ in cgs units. The break energy is then given by

$$E_b = [2a + (D/3) - 1](c_1 B_0 t)^{-1}(t/t_0)^{2a} \propto R^{2a-1} . \tag{A2}$$

Here t is time, with t_0 corresponding to the time at which the radius is R_0. This leads to a break ν_b in the synchrotron spectrum, above which the spectrum steepens from $\alpha = \alpha' = -(s' - 1)/2$ to $\alpha = \alpha' - 0.5 = -s'/2$:

$$\nu_b \approx 4.2 \times 10^9 B E_b^2 \text{ GHz} \propto R^{3a-2} . \tag{A3}$$

We see from expression (A1) that $k = (1 + Q)$ and $\alpha = -0.7$ for $s' = 2.4$ and $\nu \ll \nu_b$, while $k = (2a + Q)$ and $\alpha = -1.2$ for $s' = 2.4$ and $\nu \gg \nu_b$. It is apparent that the latter regime applies to the flaring component of 3C 273 if the steeper spectrum of this component relative to the quiescent emission is the result of synchrotron losses. The empirical result $k = 3$ derived above for $a = 1$ therefore corresponds to $Q \approx 1$, while for $a = 2$ we obtain $Q \approx 1.4$. This model therefore reproduces the observed early behavior of the outburst if there is constant injection of magnetic field and injection of relativistic electrons which increases linearly with source radius.

For the later epochs, the flux density at the turnover S_m is nearly independent of ν_m. Furthermore, the continued decrease of ν_m with time implies that the source continued to expand throughout this period. From expression (3), we find that $S_m \sim$ constant if $k = a = 1$, which implies $Q = -1$, i.e., if there is constant injection of magnetic field and injection of electrons which is inversely proportional to the source radius. The values $k = 3$, $a = 2$ would also give the desired result; this would imply that injection of magnetic field energy ceases while injection of electrons continues with $Q = 1$.

Compton losses of the electrons off the synchrotron photons can also result in the required steepening of the spectral slope by an additive factor of 0.5 if electrons are continuously injected into the source. Compton losses are notoriously difficult to include in variable-source theory, since the electron energy distribution depends on the photon density, which in turn depends on the electron energy distribution. We can, however, include Compton losses if we assume, as above, that all parameters vary as power laws with repect to the source radius, and if we make some reasonable approximations.

The Compton energy losses are given by (e.g., Pacholczyk 1970)

$$\frac{dE}{dt} = -8\pi c_1 u_{\text{ph}} E^2 ,$$

where u_{ph} is the photon energy density; the photon field is assumed to be isotropic in the rest frame of the source. This holds strictly at the center of a uniform source, and we will make the approximation that it holds throughout the source. We approximate the synchrotron photon energy density to be everywhere proportional to that at the center of a uniform spherical source with sharp frequency cutoffs ν_m at the low end and ν_{max} at the high end of the spectrum:

$$u_{\text{ph}} \approx (4\pi/c) \int_{\nu_m}^{\nu_{\text{max}}} \epsilon_\nu R d\nu$$

$$\propto (3 - s)^{-1} K B^{(s+1)/2} R \nu_m^{(3-s)/2} [(\nu_{\text{max}}/\nu_m)^{(3-s)/2} - 1] , \tag{A4}$$

where ϵ_ν is the synchrotron emission coefficient and ν_m is the turnover frequency *as seen from the center of the source*. We approximate further that the term in brackets is nearly constant as the source radius changes. This is reasonable either if ν_m and ν_{max} have roughly the same dependence on radius or if, as in our case, the value of s is close to 3. The turnover frequency ν_m is given by expression (2), with x replaced by R. We therefore obtain

$$u_{\text{ph}} \propto (KR)^{7/(s+4)} B^{(3s+5)/(s+4)} \propto R^{-U} , \tag{A5}$$

© American Astronomical Society • Provided by the NASA Astrophysics Data System

1985ApJ...298..114M

where

$$U = [-7(1 + k - D) + (3s + 5)a]/(s + 4) . \tag{A6}$$

Since the Compton loss expression is identical with that for synchrotron losses with $8\pi u_{\rm ph}$ substituted for B^2, we can use the proportionalities obtained above for the case of synchrotron losses through the substitution $2a \rightarrow U$. We then find from expressions (A2), (A3), and (A1b),

$$E_b \propto R^{U-1} , \tag{A7}$$

$$v_b \propto BE_b^2 \propto R^{2(U-1)-a} , \tag{A8}$$

and

$$k = U + Q . \tag{A9}$$

By combining equations (A6) and (A9), we finally obtain

$$\begin{aligned} k &= [(s + 4)Q + (3s + 5)a + 7(D - 1)]/(s + 11) \\ &= 0.5Q + 1.1a + 0.5(D - 1) \qquad (s = 3.4) . \end{aligned} \tag{A10}$$

If $a = 2$, the empirical value $k \approx 5.4$ requires $Q > 6$, which is quite extreme. For $a = 1$, the empirical value $k \approx 3$ can be obtained for $Q \approx 5 - D$, which is still rather extreme. For later epochs, when $S_m \sim$ const., more realistic values of Q are obtained ($Q \approx 1 - D$ for $a = 1$ and $Q \approx 3 - D$ for $a = 2$).

APPENDIX B

RELATIVISTIC SHOCK STRENGTHS

The strong shock condition can be expressed as either

$$p_2 \gg [\hat{\gamma}_1/(\hat{\gamma}_1 - 1)]p_1$$

or

$$(\Gamma'_2 - 1) \gg (\hat{\gamma}_2 - 1)^{-1}[p_1/(\rho_1 c^2)]\{1 + \hat{\gamma}_1 p_1/[(\hat{\gamma}_1 - 1)\rho_1 c^2] - 1\} \tag{B1}$$

(Blandford and McKee 1976). Here the subscript 1 corresponds to the unshocked jet plasma, and the subscript 2 to the shocked material; $\hat{\gamma}$ is the adiabatic index ($\hat{\gamma} = 4/3$ for a totally relativistic gas and $\hat{\gamma} = 13/9$ for a gas with relativistic electrons and nonrelativistic protons ["semirelativistic" gas]; e.g., Königl 1980]; p is the pressure; ρ is the rest-mass density; and the prime refers to the frame in which the undisturbed gas is at rest. Γ_2 is the Lorentz factor of the shocked gas; the Lorentz factor of the shock front is related to Γ_2 by the equation

$$\Gamma'^2_s = \frac{(\Gamma'_2 + 1)[\hat{\gamma}^2(\Gamma'_2 - 1) + 1]^2}{\hat{\gamma}_2(2 - \hat{\gamma}_2)(\Gamma'_2 - 1) + 2} \tag{B2}$$

(Blandford and McKee 1976). If the unshocked jet material moves at Lorentz factor Γ_j in the unprimed ("lab") frame, the Doppler formula gives

$$\Gamma_i = \Gamma'_i \Gamma_j (1 + \beta'_i \beta_j) \tag{B3a}$$

and

$$\Gamma'_i = \Gamma_i \Gamma_j (1 - \beta_i \beta_j) . \tag{B3b}$$

If the unshocked plasma is totally relativistic, the strong shock criterion becomes $(\Gamma'_2 - 1) \gg 0.75$, while if it is semirelativistic ($\hat{\gamma}_1 = 13/9$), we obtain $(\Gamma'_2 - 1) \gg 1.4(1 + \chi)^{-1}$, where $\chi \equiv \rho_1 c^2/p_1$. For the case of 3C 273, $s = 2.4$, hence the relativistic electron energy density is dominated by electrons at the lowest energies, probably in the 10–100 MeV range. If the protons have a similar energy distribution and low-energy cutoff, we find $\chi \sim$ 10–100. We therefore reduce the strong shock criterion approximately to $(\Gamma'_2 - 1) \gg 0.01$–0.1. If we assume that the Lorentz factor Γ_j of the undisturbed jet flow lies in the range 2–10, we find that in the "lab" frame Γ_2 must be significantly greater than 1.2–1.6 times Γ_j for the strong shock condition to be satisfied. The "lab" frame Lorentz factor of the shock front Γ_s, given by equations (B2) and (B3a), must then be much greater than 1.3–1.7 times Γ_j. The observed motion of the leading edge of the brightness enhancement generated by the shock is governed by Γ_s, which may vary from one shock to the next and which must significantly exceed the Lorentz factor of the general flow of the jet. However, if the jet component is to have a flux density comparable to that of the shocks, as we have proposed for 3C 273, we cannot allow the inequality $\Gamma_s \gg \Gamma_j$ to hold. We therefore conclude that we must allow for shocks which are only "moderately strong," in the sense that condition (B1) holds only marginally.

© American Astronomical Society • Provided by the NASA Astrophysics Data System

1985ApJ...298..114M

REFERENCES

Aller, H. D., and Aller, M. F. 1982, in *Low Frequency Variability of Extragalactic Radio Sources*, ed. W. D. Cotton and S. R. Spangler (Green Bank: National Radio Astronomy Observatory), p. 105.
———. 1984, in *VLBI and Compact Radio Sources*, ed. R. Fanti, K. Kellermann, and G. Setti (Dordrecht: Reidel), p. 119.
———. 1985, preprint.
Altschuler, D. R., and Wardle, J. F. C. 1976, *Mem. R.A.S.*, **82**, 1.
———. 1977, *M.N.R.A.S.*, **179**, 153.
Andrew, B. H., MacLeod, J. M., Harvey, G. A., and Medd, W. J. 1978, *A.J.*, **83**, 863.
Backer, D. C. 1984, in *IAU Symposium 110, VLBI and Compact Radio Sources*, ed. R. Fanti, K. Kellermann, and G. Setti (Dordrecht: Reidel), p. 31.
Bartel, N., Ratner, M. I., Shapiro, I. I., Herring, T. A., and Corey, B. E. 1984, in *IAU Symposium 110, VLBI and Compact Radio Sources*, ed. R. Fanti, K. Kellermann, and G. Setti (Dordrecht: Reidel), p. 113.
Biretta, J. A., Cohen, M. H., Unwin, S. C., and Pauliny-Toth, I. I. K. 1983, *Nature*, **306**, 42.
Blandford, R. D. 1979, in *Particle Acceleration Mechanisms in Astrophysics*, ed. J. Arons, C. Max, and C. McKee (New York: American Institute of Physics), p. 333.
Blandford, R. D., and Königl, A. 1979, *Ap. J.*, **232**, 34.
Blandford, R. D., and McKee, C. F. 1976, *Phys. Fluids*, **19**, 1130.
Blandford, R. D., and Rees, M. J. 1974, *M.N.R.A.S.*, 395.
———. 1978, in *Pittsburgh Conference on BL Lac Objects*, ed. A. M. Wolfe (Pittsburgh: University of Pittsburgh Press), p. 328.
Clegg, P. E., *et al.* 1983, *Ap. J.*, **273**, 58.
Cotton, W. D., *et al.* 1980, *Ap. J. (Letters)*, **238**, L123.
Epstein, E. E., Fogarty, W. G., Mottmann, J., and Schneider, E. 1982, *A.J.*, **87**, 449.
Gear, W. K., *et al.* 1984, *Ap. J.*, **280**, 102.
Gear, W. K., *et al.* 1985*a*, *Ap. J.*, **291**, 511.
Gear, W. K., *et al.* 1985*b*, *Ap. J.*, submitted.
Halpern, J. 1982, Ph.D. thesis, Harvard University.
Jones, T. W. 1982, *Bull. AAS*, **14**, 963 (Abstr.).
Jones, T. W., and O'Dell, S. L. 1977, *Astr. Ap.*, **61**, 291.
Jones, T. W., O'Dell, S. L., and Stein, W. A. 1974, *Ap. J.*, **188**, 353.
Jones, T. W., Rudnick, L., Aller, H. D., Aller, M. F., Hodge, P. E., and Fiedler, R. L. 1985, *Ap. J.*, **290**, 627.
Kardashev, N. I. 1962, *Soviet Astr.—AJ*, **6**, 317.
Kellermann, K. I., and Pauliny-Toth, I. I. K. 1981, *Ann. Rev. Astr. Ap.*, **19**, 373.
Königl, A. 1980, *Phys. Fluids*, **23**, 1083.
———. 1981, *Ap. J.*, **243**, 700.
Lind, K. R., and Blandford, R. D. 1985, *Ap. J.*, **295**, 358.
Malkan, M., and Sargent, W. L. W. 1982, *Ap. J.*, **254**, 22.
Marscher, A. P. 1980, *Ap. J.*, **235**, 386.
———. 1982, in *Low Frequency Variability of Extragalactic Radio Sources*, ed. W. D. Cotton and S. R. Spangler (Green Bank: National Radio Astronomy Observatory), p. 83.
Moore, R. L., Readhead, A. C. S., and Bååth, L. 1983, *Nature*, **306**, 44.
Neugebauer, G., Oke, J. B., Becklin, E. E., and Mathews, K. 1979, *Ap. J.*, **230**, 79.
O'Dea, C. P., Dent, W. A., and Balonek, T. J. 1984, in *Proc. Manchester Meeting on Active Galactic Nuclei*, ed. J. E. Dyson (Manchester: Manchester University Press), in press.
Owen, F. N., Porcas, R. W., Mufson, S. L., and Moffett, T. J. 1978, *A.J.*, **83**, 685.
Pacholczyk, A. G. 1970, *Radio Astrophysics* (San Francisco: Freeman).
Pacini, F., and Salvati, M. 1973, *Ap. J.*, **186**, 249.
Pauliny-Toth, I. I. K., and Kellermann, K. I. 1966, *Ap. J.*, **146**, 634.
Peterson, F. W., and Dent, W. A. 1973, *Ap. J.*, **186**, 421.
Petre, R., Mushotzky, R. F., Krolik, J. H., and Holt, S. S. 1984, **280**, 499.
Primini, F. A., *et al.* 1979, *Nature*, **278**, 234.
Readhead, A. C. S., Cohen, M. H., Pearson, T. J., and Wilkinson, P. N. 1978, *Nature*, **276**, 768.
Rees, M. J. 1967, *M.N.R.A.S.*, **135**, 345.
Rees, M. J. 1978, *M.N.R.A.S.*, **184**, 61P.
———. 1984, in *IAU Symposium 110, VLBI and Compact Radio Sources*, ed. R. Fanti, K. Kellermann, and G. Setti (Dordrecht: Reidel), p. 207.
Reynolds, S. P., and Chevalier, R. A. 1984, *Ap. J.*, **278**, 630.
Robson, E. I., *et al.* 1983, *Nature*, **305**, 194.
Shields, G. A. 1978, *Nature*, **272**, 706.
Unwin, S. C., Cohen, M. H., Biretta, J. A., Pearson, T. J., Seielstad, G. A., Walker, R. C., Simon, R. S., and Linfield, R. P. 1985, *Ap. J.*, **289**, 109.
van der Laan, H. 1966, *Nature*, **211**, 1131.
Wardle, J. F. C. 1977, *Nature*, **269**, 563.
Worrall, D. M., Mushotzky, R. F., Boldt, E. A., Holt, S. S., and Serlemitsos, P. J. 1979, *Ap. J.*, **232**, 683.
Zamorani, G., Giommi, P., Maccacaro, T., and Tananbaum, H. 1984, *Ap. J.*, **278**, 28.

WALTER K. GEAR: School of Physics and Astronomy, Lancashire Polytechnic, Preston PR1 2TQ, England, UK

ALAN P. MARSCHER: Department of Astronomy, Boston University, 725 Commonwealth Avenue, Boston, MA 02215

© American Astronomical Society • Provided by the NASA Astrophysics Data System